Assessing fit of individuals to group-derived structural equation models of resting-state fMRI data

G. A. James[1], R. C. Craddock[1], M. E. Kelley[2], P. E. Holtzheimer[3], B. Dunlop[3], C. Nemeroff[3], H. S. Mayberg[3], and X. P. Hu[1]

[1]Biomedical Engineering, Emory University / Georgia Institute of Technology, Atlanta, GA, United States, [2]Biostatistics and Bioinformatics, Emory University, Atlanta, GA, United States, [3]Psychiatry and Behavioral Sciences, Emory University, Atlanta, GA, United States

INTRODUCTION

Structural equation modeling (SEM) of resting state positron emission tomography (PET) data can predict how patients with major depressive disorder (MDD) will respond to treatment [1]. Specifically, variations within frontolimbic connectivity can predict whether subjects will respond to cognitive-behavioral therapy (CBT), pharmacologic intervention, or neither. Unfortunately, these previous findings are constrained to generalizations of group-level results, since the invasiveness of PET imaging limits the amount of data safely acquired per subject. To circumvent this limitation, we acquired resting-state fMRI data from 46 never-treated MDD patients. By taking advantage of FMRI's high temporal resolution, we are able to directly compare models generated for individual subjects with those generated for the entire group.

METHODS

Image Acquisition and Preprocessing: Forty-six (22 male; mean ± sd age = 42 ± 12 years old) never treated patients meeting DSM IV criteria for a current major depressive episode were recruited in accordance with Institutional Review Board policy. For the resting-state scan, participants were instructed to passively view a fixation cross while clearing their minds of any specific thoughts. MRI data acquisition was performed using a 3.0T Siemens Magnetom Trio scanner (Siemens Medical Solutions USA; Malvern PA, USA) with the Siemens 12-channel head matrix coil. Anatomic images were acquired at 1x1x1 mm^3 resolution with an MPRAGE sequence using the following parameters: FOV 224x256x176 mm, TR 2600ms, TE 3.02ms, FA 8^o. Functional data were acquired with a z-saga sequence to minimize sinal ablation of orbitofrontal cortex signal [2]. The z-saga sequence had scan parameters of FOV 220x220x80 mm, 20 axial slices, TR 2020ms, TE^1/TE^2 30ms/66ms, FA 90^o for 210 acquisitions across 7.2 minutes at 3.4x3.4x4.0mm resolution. Functional data were preprocessed as follows: slice timing correction, motion correction, written to ICB452 space using the parameters calculated from the corresponding anatomic image, temporally bandpass filtered (0.009Hz to 0.08 Hz), and spatially smoothed with a 6mm FWHM Gaussian kernel. The regions of interest (ROIs) described in [1] were anatomically defined as 6mm radius spheres atop the ICB452 MRI template. ROI timecourses were generated by calculating the mean intensity of voxels within each ROI at each timepoint. Timecourses were concatenated across subjects for group analyses.

Analysis: An exploratory adaptation of SEM [3] found the model that best fit the patient sample. This adaptation is a brute force approach that evaluated every model nested within the model proposed by Seminowicz and colleagues [1]. Next, poorly fitting models were excluded (i.e. models with parsimonious goodness of fit <0.10, path weights whose 90% confidence interval included 0, or root mean squared error of approximation (RMSEA) significantly differing from 0). Finally, these models were ranked by greatest amount of variance expained (i.e. least significant *psi* t-score), greatest number of ROIs included in model, lowest standardized root mean residual (stRMR), and highest adjusted and parsimonious goodness of fit (AGFI and PGFI).

RESULTS AND DISCUSSION

Figure 1 shows the base model (from [1]) and refined model generated from exploratory SEM of MDD patients' resting-state fMRI data. None of the approximately 130,000 possible models could adequately explain thalamic variability. This finding is unsurprising, given that thalamus had only one possible path (thalamus to MACC24) through which its variance could be explained. The absence of DLPF9 in the final model is unexpected; while this may reflect symptology, a more rigorous approach to ROI definition is warranted before drawing such conclusions.

Of considerable interest is how individual patients fit the group model. The group model was evaluated for each patient, and the individuals' path weights were plotted as histograms. Figure 2 shows two histogram extremes; one path (MACC24 to OFC11) where individuals' path weights have a Gaussian distribution and are centered about the group value, and another path (MACC24 to MPF10) where the distribution of individuals' path weights are not Gaussian and not centered about the group value. These histograms respectively demonstrate what patients share in common and what may discriminate them into subgroups. Future elaboration of this work, with a larger sample size and more extensive ROI selection, may prove capable of discriminating between responders and nonresponders or even predicting patient response to different treatments.

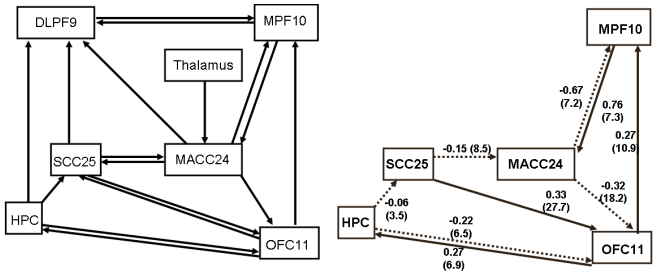

Figure 1. Base model (left) generated from PET ([1]) and final model (right) generated from fMRI and refined with exploratory SEM. SCC25: subgenual cingulate (MNI coord 1 -24 -10); MACC24: midanterior cingulate (1 -17 -34); HPC: hippocampus (-29 24 -12), DLPF9: dorsolateral prefrontal cortex (-34 -48 27); MPF10: medial prefrontal cortex (1 -62 14); OFC11: orbitofrontal cortex (1 -49 -10), Thalamus (-14 3 7).

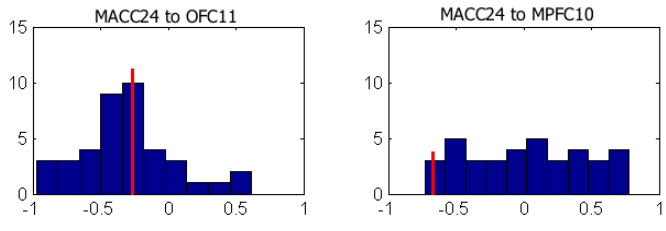

Figure 2. Histograms of individual subjects' path weights for MACC24 to OFC11 (left) and MPFC10 (right). MACC24 to OFC11 has an approximate Gaussian distribution centered about the group path value, suggesting that it better represents group membership than the MACC24 to MPFC10 path, which is neither Gaussian distributed nor centered about the group value.

ACKNOWLEDGEMENTS. This work was supported in part by NIMH P50 MH077083 and NIBIB RO1EB002009.

REFERENCES . [1] Seminowicz et al, NeuroImage 2004. [2] Heberlein and Hu, MRM 2004. [3] Zhuang et al, NeuroImage 2005.